A novel Monte Carlo Simulation for Molecular Interactions and Diffusion in Postsynaptic Spines

Yoshihisa Kubota[1], Tara R. Gaertner[1], John A. Putkey[2] and M. Neal Waxham[1]
[1]Department of Neurobiology and Anatomy, and [2]Biochemistry and Molecular Biology, University of Texas Medical School, Houston, Texas 77030, USA

Abstract
We developed a new Monte Carlo simulator that can incorporate anomalous diffusion and chemical kinetics of intracellular signaling molecules in the dendritic spine. The simulator is based on two well-established Monte Carlo approaches, namely the Kopelman algorithm and the Kinetic Monte Carlo algorithm. This paper describes the basic features of the simulator and compares its performance for the general case of elementary chemical reactions. We then explore anomalous diffusion of calmodulin (CaM) in the dendrite. The simulations suggest that the CaM-binding protein RC3 plays a significant role in determining the spatio-temporal dynamics of CaM-target interaction.

***Keyword*:** Monte Carlo simulation; anomalous diffusion; range of action; calmodulin; dendritic spine

1. Introduction
Increased intracellular Ca^{2+} is required for the induction of synaptic plasticity, both long-term depression (LTD) and long-term potentiation (LTP). The distinction between LTP and LTD has long been hypothesized to do with how the distribution of Ca^{2+} in space and time within the spine compartment regulates downstream signaling machinery.

Computer simulations are useful tools to examine this hypothesis. However, they are presently complicated by several factors. First, the number of molecules involved in signaling pathways within the spine is small. Second, cytoplasm is a complex milieu and signaling molecules are not randomly distributed. They may undergo chemical kinetics as well as diffusion very different from those observed in an ideal solution [1, 2].

These features demand that chemical reactions and diffusion of signaling molecules be computed individually. Monte Carlo approaches are currently the only computational strategy capable of efficiently incorporating these two key features of synaptic signaling. MCell (http://www.mcell.cnl.salk.edu) attempts to incorporate some of these features as highlighted in recent papers [3, 4]. Nevertheless, the current version of MCell cannot compute interactions between two freely diffusing molecules.

Here we begin to address these problems by creating a new Monte-Carlo simulation by fusing features of the Kopelman algorithm for molecular interactions and the Kinetic Monte-Carlo simulation of molecular diffusion (used in surface/material science). The first part of this paper describes the algorithm's basic architecture. Second, we compare simulated results against elementary chemical kinetics. Third, we explore the range of action of Ca^{2+}-calmodulin and its modulation by a unique calmodulin-binding protein, RC3 (neurogranin). The simulations suggest that RC3 plays a significant role in determining the spatio-temporal dynamics of CaM-target interactions during Ca^{2+} oscillations.

2. Simulation Algorithm
The first step in developing our Monte-Carlo simulation was to re-examine Gillespie's original derivation of the algorithm [5]. To derive the probability of chemical reactions within a give time period, Gillespie calculated the probability of collision of two reacting

molecules and then compute the conditional probability of chemical reaction given the collision. To remove the assumption of homogeneity from the Gillespie algorithm, we need to calculate the probability of collision of two reacting molecules explicitly in a non-homogenous system. Our solution was to simulate motion of molecules by random walk. In the simulation, a collision occurs when two molecules come within a certain distance defined by the radius of the reacting molecules.

Suppose we have a pair of binding and dissociation reactions.

$$A + B \xrightarrow{k_1} C \quad (1)$$

$$C \xrightarrow{k_{-1}} A + B \quad (2)$$

where A and B may represent Ca^{2+}, CaM or RC3 in our simulation (Fig. 3). The k_1 and k_{-1} are corresponding on- and off-rates.

We simulate reaction (1) using a Monte Carlo (MC) algorithm on 3D cubic lattices with appropriate (e.g., reflective or cyclic) boundary conditions. Each molecular species (A, B and C) is mobile on the lattice through diffusion, which is modeled by independent random walks of individual molecules. At any moment of the simulation, one given lattice site cannot be occupied by more than one molecule. The probabilities f and g are set to be proportional to the corresponding rate coefficients k_1 and k_{-1} respectively (as in the Gillespie algorithm). The A and B molecules are placed on the lattice by randomly choosing their coordinates at the beginning of the simulation. The molecules are moved according to the microscopic rules that are consistent with classical reaction rate theory as well as kinetic theory of statistical physics (known as the Kopelman algorithm [6, 7]). For example, for molecule A, a destination site is chosen at random among its nearest neighbors. If this destination site is unoccupied, the A-molecule moves to it directly. If the destination site is occupied by a B molecule, a random number is chosen between 0 and 1. If this number is lower than the reaction probability f, the destination site is turned into a C molecule and the initial A site becomes unoccupied. In all other cases, the A molecule remains at its initial position.

A Monte Carlo simulation scheme, known as the BKL (Bortz-Kalos-Lebowitz) algorithm [8], provides an accurate way of generating reaction trajectories according to the correct probability distributions calculated from the lattice configurations and the above mentioned microscopic reaction rules. This is very similar to the Kinetic Monte Carlo simulation used for atomic scale surface diffusion and island growth (www.ipm.virginia.edu/research/PVD/Pubs/yang_thesis/). To establish our new algorithm, the Kopelman algorithm was rearranged and modified in the following way:

(a) Compute the individual and cumulative reactions/jump rates (= propensity function)
(b) Select a reaction/jump path according to the probability distribution
(c) Execute reaction/jump
(d) Increment time according to the cumulative propensity function
(e) Update and re-calculate the next possible reaction/jump probability
(f) Iterate step (a) through (e).

If we compute jump probabilities according to the measured diffusion coefficient, we will be able to accurately simulate molecular diffusion that precedes chemical interactions. Thus, we have created a novel interface combining the Kopelman algorithm and the

Kinetic Monte Carlo simulation. The lattices of our typical simulation (e.g., Fig. 3) contain 1 x 10^6 cubic volumes of 5 nm each side, constrained by the size of each CaM target protein as well as the spine head.

Such simulations can be computationally intensive. For the results presented below, a single desktop workstation (Pentium, 3.05 GHz) and under the Matlab environment, required ~ 60 - 70 hrs to simulate 1 second of real time of 1000 diffusing molecules that undergo diffusion and chemical reactions in the presence of 40,000 immobile obstacles. While efforts are underway to enhance simulation performance (coding in C and parallelization) even with this modest computational power, the simulation times were nor preventative for obtaining meaningful results,

3. Results & Summary

3-1 Molecular Diffusion

We have confirmed and verified our Monte Carlo simulation in several ways. One test is molecular diffusion in a 3D lattice space without obstacles. The Monte Carlo simulations are then compared to results from the analytical solution for 3D diffusion from an instantaneous point source. The solution of the diffusion equation in 3D for an instantaneous point source at the origin at time $t = 0$ is:

$$C(r,t) = \frac{N}{(4\pi Dt)^{3/2}} \exp(-r^2 / 4Dt) \tag{3}$$

where $C(r,t)$ is the expected concentration of the molecules at radial distance r at time t, N is the number of molecules that started at the point source, and D is the diffusion coefficient. Therefore, the Monte Carlo simulation should reproduce the probability density (Fig. 1A) given by:

$$P(r,t) = 4\pi r^2 dr C(r,t) \tag{4}$$

Another comparison (Fig. 1B) of the result was carried out using a log-log plot of the mean-square displacement (Equation 5). The log-log plots of the mean-square displacement against time should give rise to a straight line and the slope of the line (Eq. 6) is a widely used value to distinguish between normal ($\alpha = 1$) and anomalous diffusion ($0 < \alpha < 1$).

$$< r^2(t) >= \int_0^\infty 4\pi dr C(r,t) r^2 = 6Dt \tag{5}$$

$$\log < r^2(t) >= \alpha \log t + \log(6D) \tag{6}$$

Without obstacles, the simulation reproduces classical Brownian motion (the top line in Fig. 1B). With increasing obstacles densities, the slope of the curve becomes lower, and the diffusion becomes anomalous. These results are in agreement with previously published simulation of anomalous diffusion [7, 9].

3-2 Chemical Reaction

As a second test, the simulation must reproduce chemical kinetics in a well-stirred system. We generated a Kinetic Monte Carlo simulation of an elementary reaction:

$$A + B \rightarrow C \quad (7)$$

in a well-stirred homogeneous space and compared it with the law of mass action (Fig. 2A). These molecules (A, B and C) undergo random-walks and chemical reactions. The time evolutions of product (C) formation are computed either by the Monte Carlo algorithm or by the analytic solution. Fig 2A compares the average of 100 Monte Carlo simulations and the analytic solution, which are indistinguishable (two overlapping solid lines). Note that the dotted line represents the result of a ***single*** Monte Carlo simulation run, showing that fluctuations are relatively small and the fit is excellent for a wide range of time scales.

Our simulation contains molecules (e.g., Ca^{2+}, CaM and RC3) that each has different diffusion coefficients and they undergo chemical reactions at the same time. Fig. 2B demonstrates that our simulation algorithm does reproduce the chemical reaction between molecules with different diffusion coefficients. In this simulation, we use the same reaction conditions (Eq. 7) and the reaction probability as in Fig. 2A except the diffusion coefficient of the A-molecule is varied. The Smoluchowski's bimolecular rate constant for free diffusion without inter-particle force (e.g., Coulomb interaction) is given by:

$$k = \frac{4\pi D R_0}{1 + D / R_0 \omega} \quad (8)$$

$$D = D_A + D_B \quad (9)$$

where D_A and D_B are diffusion coefficients of A- and B- molecules, respectively. R_0 and ω are some constants derived from the boundary condition of the Smoluchowski equation. In our simulation, we set reaction rates to be very large (= 0.5/Monte Carlo step/nearest-neighbor colliding particle pair). Thus, the reaction rate is diffusion limited and the second term of the denominator of Eq. 8 for this particular simulation experiment is negligible. In other words, the reaction rate $k \sim 4\pi(D_A + D_B)R_0$ is a linear function of diffusion coefficients of A- and B-molecules. When $D_A / D_B = 0$ (A-molecules are immobile/static), the expected reaction rate is half of the original rate in which $D_A / D_B = 1$. Fig. 2 B compares the theoretical prediction (solid lines) and the average of 100 Monte Carlo simulations (dotted lines) for different D_A / D_B values. For illustration purposes, $1/(A(0) - C(t))$ is plotted as a function of time (which should give rise to a straight line) where $A(0)$ is the initial number of A- and B- molecules (= 1000) and $C(t)$ is the number of C-molecule at time t. This analysis establishes an explicit formulation of reaction probability in our Monte Carlo simulation.

3-3 Range of Action of Ca^{2+} saturated CaM

In order to gain insight into CaM's function in the spine, we calculated Ca^{2+}-CaM's range of action with the new simulator. The range of action is an estimation of the distance that CaM can travel before Ca^{2+} dissociates from it for a given Ca^{2+} concentration. This will provide a computational tool that we can use to relate detailed CaM/target interactions to the spatio-temporal dynamics of the spine molecular machinery.

We calculated CaM's range of action in the presence and absence of the CaM-binding protein RC3. RC3 (neurogranin) is enriched in dendritic spines but it has no identified

enzymatic activity, although recent knockout experiments suggested a role for RC3 in synaptic plasticity [10]. Detailed kinetic analysis showed that the rate of Ca^{2+} dissociation from the C-terminal lobe of CaM was increased by 30-fold in the presence of RC3 (k_{off} rates: from 8.5/sec to 270/sec) [11]. We therefore hypothesized that the range of action of Ca^{2+}-saturated CaM should be regulated by RC3 and simulations were done using the new simulator to examine this hypothesis.

In the absence of RC3, the range of action for CaM increases with the Ca^{2+} concentration and reaches a plateau value of 120 nm at Ca^{2+} >= 10 μM (Fig. 3). The presence of RC3, on the other hand, decreases the range of action in a RC3 concentration dependent manner and for all Ca^{2+} concentrations tested.

The synaptic spine contains many other proteins that interact with CaM (e.g., CaMKII and calcineurin). The range of action of Ca^{2+} saturated CaM may well be more complicated than presented here. Our simulation scheme, however, will provide a useful tool to further investigate this issue.

4. Conclusion

We have created a novel Monte-Carlo algorithm that accommodates molecular diffusion and chemical reactions. The simulation results agreed well against those generated from classical reaction rate theory for a well-mixed dilute chemical system. The preliminary results suggest that this new Monte Carlo simulation will provide a powerful tool to investigate spatio-temporal dynamics of the Ca^{2+}-CaM-target biochemical network in the dendritic spine.

Acknowledgements

This work was supported by NIH grant NS26086. Y.K. was supported by NIH training grant NS41226. T.R.G. was supported by a scholarship from the Natural Sciences and Engineering Research Council of Canada.

References:

[1] P. Schwille, U. Haupts, S. Maiti, W.W. Webb, Molecular dynamics in living cells observed by fluorescence correlation spectroscopy with one- and two-photon excitation. Biophys J. 77 (1999) 2251-2265.

[2] M. Wachsmuth, W. Waldeck, J. Langowski, Anomalous diffusion of fluorescent probes inside living cell nuclei investigated by spatially-resolved fluorescence correlation spectroscopy. J.Mol.Biol. 298 (2000) 677-689.

[3] K.M. Franks, T.M. Bartol, T.J. Sejnowski, An MCell model of calcium dynamics and frequency-dependence of calmodulin activation in dendritic spines. Neurocomputing 38 (2001) 9-16.

[4] K.M. Franks, T.J. Sejnowski, Complexity of calcium signaling in synaptic spines. Bioessays 24 (2002) 1130-1144.

[5] D.T. Gillespie, A Rigorous Derivation of the Chemical Master Equation. Physica A 188 (1992) 404-425.

[6] A. Lin, R. Kopelman, Argyrakis P, Nonclassical kinetics in three dimensions: Simulations of elementary A+B and A+A reactions. Physical Review E 53 (1996) 1502-1509.

[7] H. Berry, Monte Carlo simulations of enzyme reactions in two dimensions: Fractal kinetics and spatial segregation. Biophysical J. 83 (2002) 1891-1901.

[8] A.B. Bortz, M.H. Kalos, J.L. Lebowitz New Algorithm for Monte-Carlo Simulation of Ising Spin Systems. *Journal of Computational Physics* 17 (1975) 10-18.

[9] M.J. Saxton, Anomalous diffusion due to the obstacle: a Monte Carlo study. Biophys.J. 66 (1994) 394-401.

[10] T. Krucker, G.R. Siggins, R.K. McNamara, K.A. Lindsley, A. Dao, D.W. Allison, L. De Lecea, T.W. Lovenberg, J.G. Sutcliffe, D.D. Gerendasy, Targeted disruption of RC3 reveals a calmodulin-based mechanism for regulating metaplasticity in the hippocampus. J. Neurosci. 22 (2002) 5525-5535.

[11] T.R. Gaertner, J. Putlkey, M.N. Waxham, RC3/neurogranin and Ca^{2+}/calmodulin-dependent protein kinase II produce opposing effects on the affinity of calmodulin for calcium. J. Biol. Chem. (2004) in press (manuscript M405352200)

Figure Legends

Fig. 1 (A) Comparison of diffusion between the Kinetic Monte Carlo models and the Analytic Solution. A single molecule was deposited at the origin at t=0 and the simulations were repeated 2000 times. The lattice volume contains no barrier/obstacles or boundary. Crosses, open circles and diamonds represent individual data points of the particle distribution with respect to displacement at the corresponding time points. Lines represent results from the analytic solution (Eq. 4) for times t=10, 20, 50, 100 (Monte Carlo steps). **(B) Anomalous Diffusion Due to Obstacles**. The mean-square displacements of diffusing particles are plotted as a function of time (= Monte Carlo step/particle). The diffusion coefficient is the same as in (A). The densities of randomly placed obstacles are (from top to bottom): 0.0, 0.04, 0.1, 0.2, 0.3 and 0.4 (indicated by the arrows).

Fig. 2 Kinetic Monte Carlo simulation of elementary reactions $A + B \rightarrow C$ **(A)** 1000 of each A- and B- molecules were randomly placed in the lattice space at *t=0* and the reactions were simulated as described in the text. The average of 100 simulations were compared to the mean field solutions (two overlapping solid lines for each case, (relative error < 0.1 %). The dotted line is the trajectory of a ***single*** Monte Carlo simulation run. The diffusion coefficients of A and B molecules are the same. **(B)** The assigned diffusion coefficient of A molecules was varied as indicated and simulations of the binary reaction $A + B \rightarrow C$ were carried out as in (A). The diffusion coefficient of B molecules and the reaction probability are the same as in (A). The slope of the plot of $1/(A(0) - C(t))$ vs. time *t* represents the rate constant for each diffusion coefficient as indicated in the figure.

Fig. 3 Range of action of Ca^{2+}-saturated CaM. The mean distance traveled by Ca^{2+}-saturated CaM is plotted as a function of the steady-state level of Ca^{2+} concentration in a cubic lattice of 0.125 μm^3 at different concentration of RC3. From top to bottom: no RC3; 750 molecules of RC3, equivalent to 10 μM. 1500 molecules of RC3, equivalent to 20 μM. The results are the average of 50 simulation experiments. RC3 decreases the range of action for all Ca^{2+} concentrations tested. At the 20 μM of Ca^{2+}, the range of action was reduced from 120 nm (no RC3) to 20 ~ 30 nm (at 20 μM of RC3), close to the diameter of a CaMKII holoenzyme.

Fig. 1

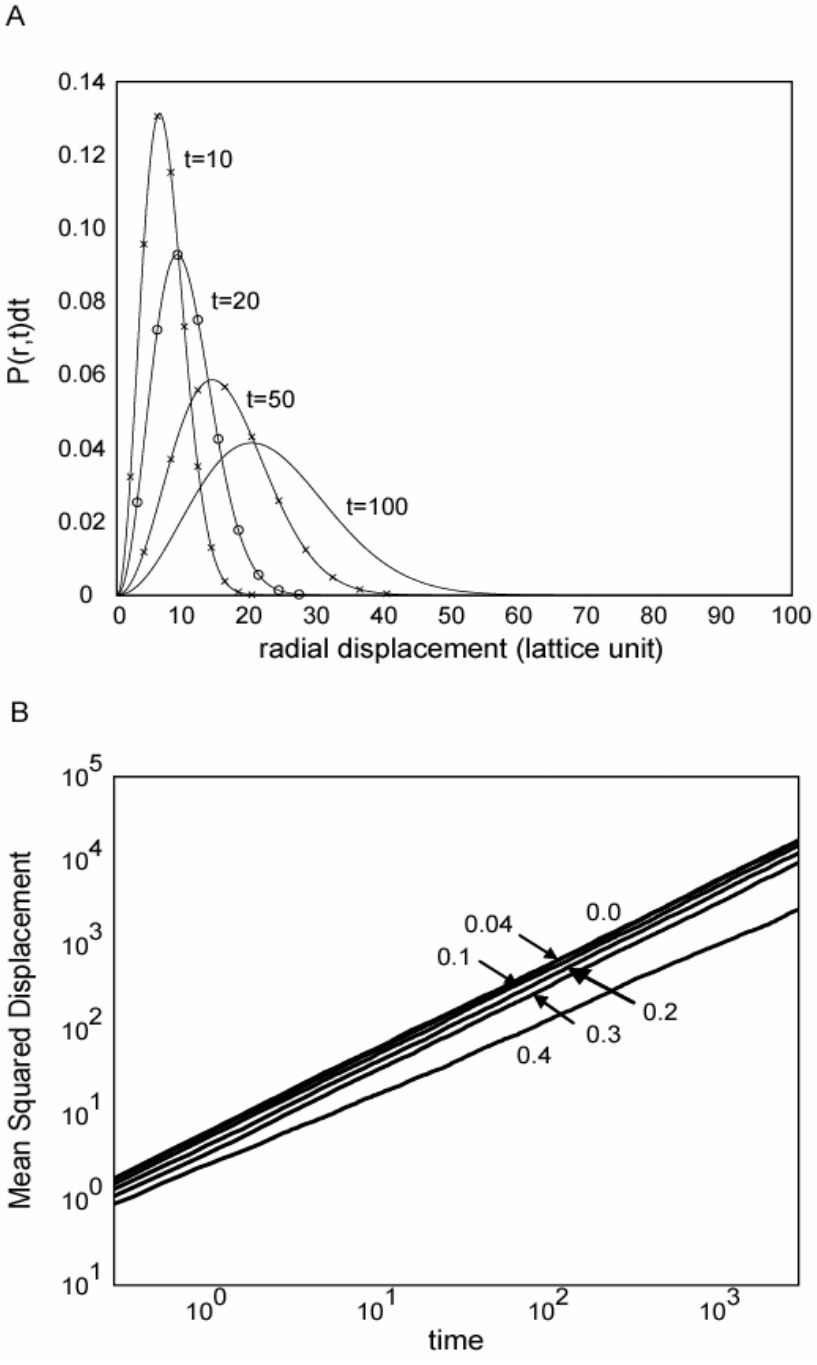
A
P(r,t)dt
radial displacement (lattice unit)
t=10
t=20
t=50
t=100
B
Mean Squared Displacement
time
0.0
0.04
0.1
0.2
0.3
0.4

Fig. 2

A

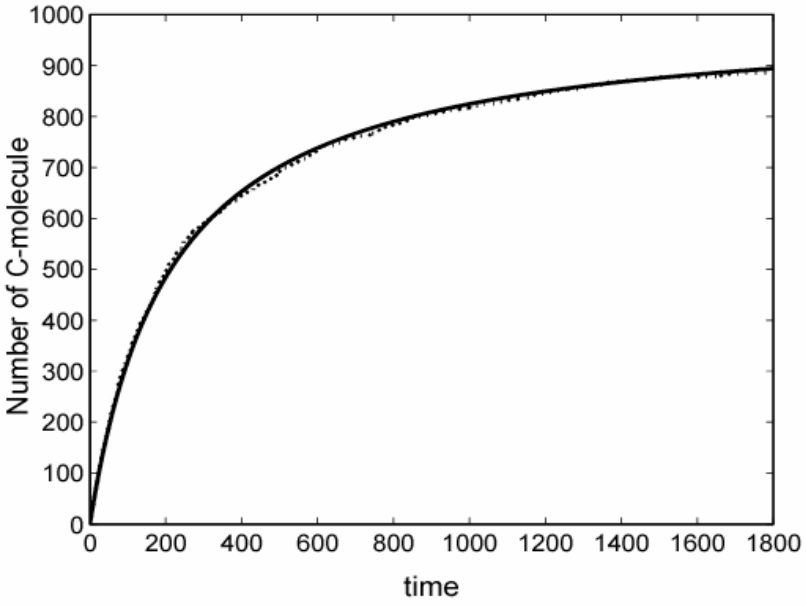
Number of C-molecule
time
0
100
200
300
400
500
600
700
800
900
1000
0
200
400
600
800
1000
1200
1400
1600
1800

B

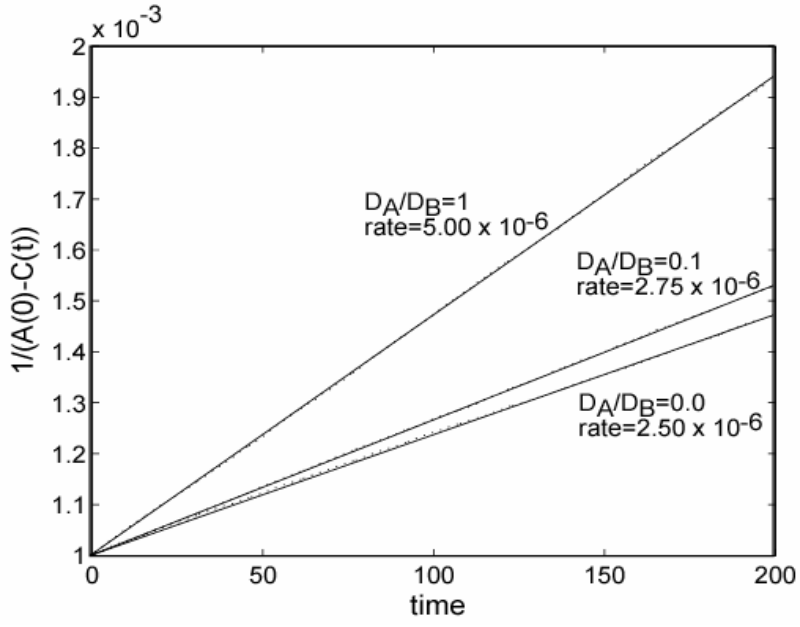
x 10^-3
1/(A(0)-C(t))
time
D_A/D_B=1
rate=5.00 x 10^-6
D_A/D_B=0.1
rate=2.75 x 10^-6
D_A/D_B=0.0
rate=2.50 x 10^-6
1
1.1
1.2
1.3
1.4
1.5
1.6
1.7
1.8
1.9
2
0
50
100
150
200

Fig. 3

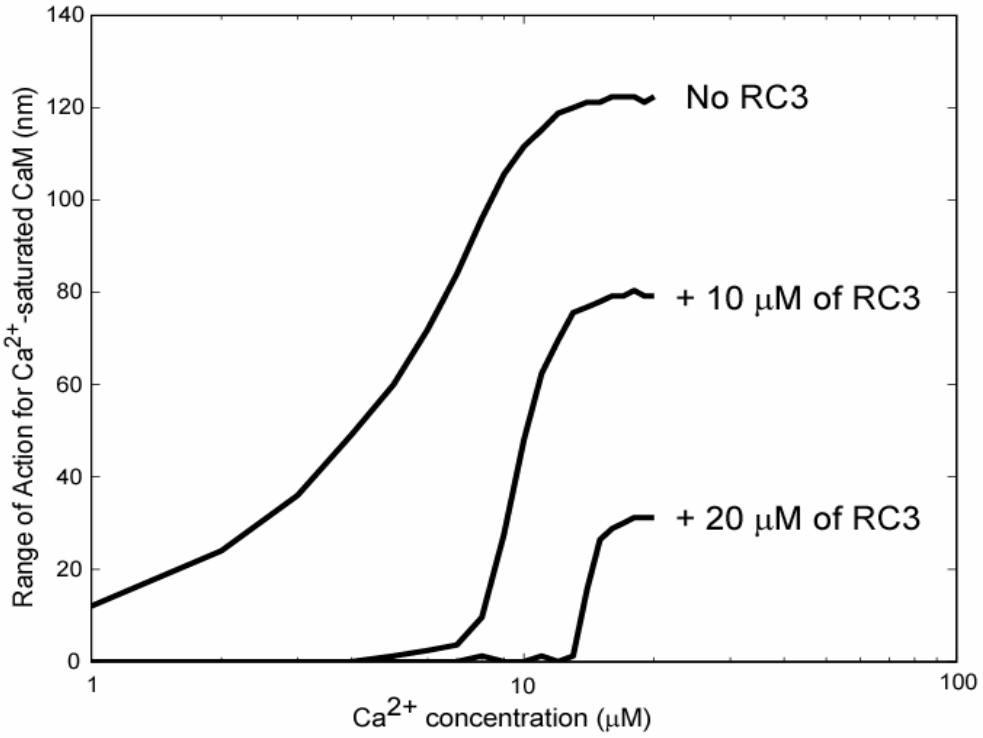
140
120
100
80
60
40
20
0
Range of Action for Ca2+-saturated CaM (nm)
No RC3
+ 10 μM of RC3
+ 20 μM of RC3
1
10
100
Ca2+ concentration (μM)